

# Design Parameters and Validation for a Non-Contacting Flux-Pinned Docking Interface

Laura L. Jones<sup>1</sup>, William R. Wilson<sup>2</sup>, and Mason A. Peck<sup>3</sup>  
*Cornell University, Ithaca, NY 14850*

Rendezvous and docking remains one of the most important but also the most difficult and dangerous maneuvers commonly required of spacecraft. We propose the use of magnetic flux pinning as a close range augmentation to current docking practices. As an interaction between a magnetic field and a type II superconductor, flux pinning forms a non-contacting equilibrium that can be used to attach multiple spacecraft. We describe the components necessary to form a flux pinned interface and how it could be implemented as a docking augmentation in several stages of the maneuvers. Also discussed are some of the important parameters necessitating optimization for implementation of a FPI as docking augmentation. A model of flux-pinned docking is presented that predicts the behavior of such a system on small nanosatellite modules. Simulation results using parameters from flux-pinned docking system on a microgravity flight hardware based on this model illustrate the performance of the FPI under a variety of conditions.

## Nomenclature

|                            |   |   |
|----------------------------|---|---|
| $\hat{\mathbf{a}}$         | = | superconductor surface normal                                       |
| $\mathbf{B}_{tot}$         | = | total ambient magnetic field  |
| $\mathbf{B}_{frozen}$      | = | ambient magnetic field due to the frozen image                      |
| $\mathbf{B}_{mobile}$      | = | ambient magnetic field due to the mobile image                      |
| $c$                        | = | linear damping coefficient  |
| FPI                        | = | flux-pinned interface   |
| $g$                        | = | gravitational acceleration  |
| $[\mathbf{I}]_i$           | = | inertia matrix of a magnet  |
| $k_d$                      | = | derivative gain   |
| $k_i$                      | = | integral gain   |
| $k_p$                      | = | proportional gain   |
| $\mu_0$                    | = | permeability of free space  |
| $\mathbf{n}$               | = | dipole moment vector  |
| $\mathbf{n}_{FC,i}$        | = | dipole moment vector of magnet $i$ at field-cooling                 |
| $\hat{\mathbf{n}}$         | = | dipole moment unit vector $\mathbf{n}/ \mathbf{n} $                 |
| $\mathbf{r}$               | = | inertial position vector  |
| $\boldsymbol{\rho}$        | = | relative position vector from the image to its source               |
| $\boldsymbol{\rho}_{m_i}$  | = | relative position vector of a mobile image to its source magnet $i$ |
| $\boldsymbol{\rho}_{f_i}$  | = | relative position vector of a frozen image to its source magnet $i$ |
| $\boldsymbol{\rho}_{1f_2}$ | = | relative position vector of magnet 1's frozen image to magnet 2     |

<sup>1</sup> Graduate Student, Dept. of Mechanical and Aerospace Engineering, 129 Upson Hall Ithaca NY 14853, AIAA Student Member.

<sup>2</sup> Graduate, Dept. of Mechanical and Aerospace Engineering, 129 Upson Hall Ithaca NY 14853, AIAA Student Member.

<sup>3</sup> Assistant Professor, Dept. of Mechanical and Aerospace Engineering, 212 Upson Hall Ithaca NY 14853, AIAA Full Member.

## I. Introduction

**A**LTHOUGH spacecraft have been successfully docking since 1966, this maneuver remains one of the most complex and difficult tasks performed on orbit. The risk of collision is always present; equipment worth many millions of dollars and even human lives may be at stake. As a result, research into docking procedures places a heavy emphasis on ensuring that the system is inherently stable and safe even in the case of a loss of control or. Alternatively, if system stability is not achievable, a satisfactory collision avoidance maneuver must be computed at each point during the maneuver.<sup>1</sup> The need for such highly constrained trajectories limits efforts to optimize these paths for fuel consumption, time, and other factors. However, recently developed applications for a technology known as a flux-pinned interface offers an innovative solution consistent with many of these constraints. This technology establishes a passive, non-powered, stable equilibrium between a docking pair of satellites using a phenomenon in superconducting physics known as flux pinning.

Magnetic flux pinning is a non-contacting interaction between magnetic fields and superconductors that has been studied primarily for its levitating ability on Earth's surface<sup>2</sup>, but ongoing research has been investigating its suitability for a variety of spacecraft applications such as reconfiguration, close-proximity formation flying, and docking.<sup>3,4</sup> Flux pinning exhibits high stiffness and damping over a range defined by the strength of the magnetic field. Flux pinning stiffness is sufficient to resist many perturbations commonly found in the space environment.<sup>3</sup>

An array of superconductors and magnets on the spacecraft of interest make up a flux-pinned interface, or FPI. One can influence the properties of the FPI by manipulating the magnetic fields. The FPI can maintain an equilibrium position in all six degrees of freedom, and may be turned off at will. Provided the superconductor remains below its critical temperature, no power is required to activate or maintain this connection – a restoring force preventing a collision will be in place even in the event of a loss of control, without the need for intervention from ground stations.

Flux pinning interactions in a microgravity environment have been successfully demonstrated and at least partially characterized for CubeSat-scale spacecraft mockups.<sup>5</sup> However, because of the novelty of this technology, no basis of comparison exists to determine its performance and other fundamental characteristics as a docking augmentation method. Testbeds such as the FloatCubes developed at Cornell University will allow more thorough characterization of the properties of FPIs for a variety of applications, including docking.<sup>6</sup> The research group is also currently pursuing an opportunity to fly CubeSat-scale spacecraft mockups on a microgravity flight in late September through NASA's FAST 2010 program. This paper presents a more complete picture of the forces, masses, and couplings involved in a FPI interaction by compiling previous published work and simulation validations. Section II describes a Flux-Pinned Docking Interface by explaining the physics involved, explaining how these physics might apply to various points along the rendezvous maneuvers, and design parameters to consider in the design of such an interface. The second section describes in detail a nonlinear model for the system and shows simulation results based on these models and system parameters from the RAGNAR project hardware. The paper concludes with a summary of the pertinent aspects of the flux-pinned docking interface and an assessment of its potential for improving docking technology.

## II. Flux-Pinned Docking Interface

### A. Flux Pinning Background

Magnetic flux pinning is an interaction that occurs between a strong magnetic fields and type II superconductors. Flux pinning occurs when magnetic fields are trapped in material impurities in the superconductor, inducing current vortices which resist change to the magnetic flux distribution.<sup>7</sup> Flux pinning occurs only below a material-dependent critical temperature  $T_C$ , which is approximately 80 K for high-temperature superconductors (HTSCs) such as YBCO that are commonly used for flux pinning. When the HTSC is cooled below  $T_C$  in the presence of a strong magnetic

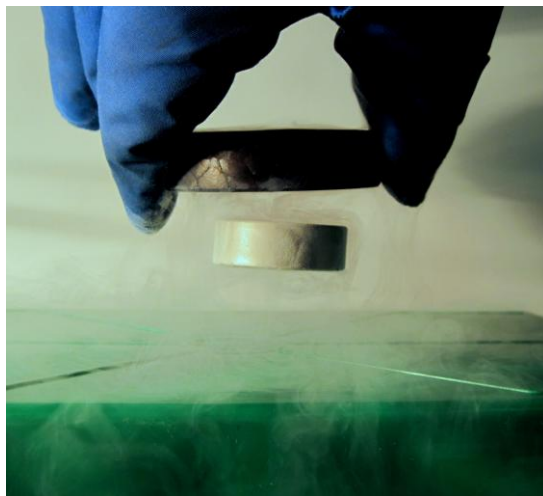


**Figure 1. A Neodymium magnet (below) flux pinned to a YBCO disc (above), shown levitating in 1-g. The YBCO was cooled below its critical temperature of 88 K using a bath of liquid nitrogen.**

field, the magnetic flux is captured by the superconductor, imprinting the relative position and orientation of the magnet into the superconductor's material. The magnetic field source is pinned to the superconductor so that the interface resists perturbations from the equilibrium via a nonlinear restoring force.<sup>8</sup>

The process of establishing the FPI by bringing the HTSC below its critical temperature is known as field cooling and forms the basis for the FPI.<sup>9,10</sup> Once the FPI is established, the equilibrium between magnet and HTSC is passively stable, requiring no active control or added energy (in the case of permanent magnets) to keep the system in the established equilibrium arrangement.<sup>3</sup> One common application of flux pinning is magnetic levitation in 1 g, as shown in Figure 1. A flux-pinned interface can exhibit stiffness and damping in six degrees of freedom (6DOF), resisting any relative motion of the system components from the established equilibrium position. This is due to the superconductor resisting any change in the magnetic flux it has pinned. With an axisymmetric field, however, some DOFs can be left unconstrained. With magnetic field symmetry, the HTSC does not detect any change when the magnet rotates in that DOF and therefore does not resist this motion. This behavior allows the potential for FPIs to function as non-contacting mechanisms. For example, when a symmetric magnetic field is generated by one spacecraft module and a superconductor flux-pinned to it is mounted on another module, the FPI can function as a revolute joint. Previous work in this area<sup>3,11, 12</sup> has confirmed that flux pinning can create joints and other mechanisms, some of which have been validated in both laboratory experiments and during microgravity testing.<sup>13</sup> These mechanisms, when deployed as links on a close formation of spacecraft modules, could allow the spacecraft to easily reconfigure via ground-based commands to electromagnets.

## **B. Rendezvous and Docking with Flux Pinning**

A typical spacecraft mission involving docking can be divided into five major phases<sup>1</sup>:

1. Launch
2. Phasing
3. Far range rendezvous
4. Close range rendezvous
5. Mating

As flux pinning can generally be used on the scale of the augmented spacecraft's length, it can best be applied to this sequence during the close range rendezvous segment. Flux pinning can in some cases also provide an ideal mating solution as well, as in the case of a frequently reconfiguring modular spacecraft that does not require physical connections between modules.

Flux pinning can be used during the close approach phase of docking to improve currently used procedures. A typical docking process, as described in Fehse 2003<sup>1</sup>, involves several stages of maneuvering at close range to complete the docking sequence, some of which are listed below:

- 1.Reduction of approach velocity and misalignments
- 2.Reception
- 3.Impact attenuation
- 4.Capture
- 5.Retraction and Structural Alignment
- 6.Structural Connection

Once the spacecraft are in close proximity, they must first reduce relative velocity and misalignment of their docking interface. As the craft close to the range of a few meters, they must achieve alignment to place the docking interface within reception range. In the reception phase, the docking interfaces of the two spacecraft enter each other's reception range, the range in which physical contact of the spacecraft is possible. Before physical contact can be made, the relative velocity between the craft must be reduced. This reduces the impact shock between the vehicles when contact is made, decreases rebound velocity, and increases time available for the capture process. Once reception and impact attenuation have been accomplished, the capture structures of the docking interface can engage, preventing the two vehicles from escaping from each other. After capture, the spacecraft must be aligned so that a structural connection can be made. This connection must provide stiffness to keep the vehicles together under any loading conditions the system can experience.

Current docking routines, such as those employed on the European Space Agency's Autonomous Transfer Vehicle, or ATV, employ primarily visual sensors at close range. The ATV uses multiple onboard visual sensors in conjunction with visual data from the International Space Station.<sup>14</sup> Despite the computing effort and active control guiding visual-based docking, it is an inherently difficult and dangerous process because strategies are vulnerable to loss of communications, power failures, and unpredicted errors that affect the control system. One example of such a failure was the 2005 Demonstration of Autonomous Rendezvous Technology (DART) project, which attempted to autonomously rendezvous with a satellite, but due in part to erroneous navigational code instead collided with its target.<sup>15</sup> This failure during a technology demonstration of actively controlled docking demonstrates the need for a more robust method of accomplishing spacecraft docking.

Flux pinning can be used to accomplish some or all of these docking stages, as is illustrated in Figure 2. In a simple example, the target spacecraft would mount a superconductor with a pinned image as part of its docking interface, while the approaching vehicle would have a permanent magnet that matches the pinned image. As the spacecraft enter the range where magnetic fields can significantly affect their interactions, flux pinning can bring the two craft to a known, safe relative equilibrium. The magnet on the approach vehicle will seek the distance and alignment of the pinned image in the superconductor, performing a reduction of the system's relative velocity and misalignment. Provided that the preset equilibrium position is within reception range, the vehicles will also be passively drawn into reception. The damping present in flux pinning interactions can provide significant impact attenuation between the spacecraft. With correctly chosen magnets and superconductors, the flux-pinned interface will bring the relative velocity and misalignment between vehicles to zero and leave them in a known and passively stable equilibrium position. So long as the pinning is maintained, this equilibrium can serve as the capture of the spacecraft.

The addition of an electromagnet to the approaching spacecraft can extend the use of flux pinning to the retraction and structural alignment phase of the docking sequence. The electromagnet can provide fine actuation of the established flux-pinned equilibrium position. It can be used to bring the craft closer together or to reorient the craft to a more convenient alignment, providing any needed retraction and structural alignment. For spacecraft needing to physically connect, they can now deploy physical docking apparatus. Modular spacecraft, with segments that do not require physical contact, can rely on the established flux pinning to maintain connectivity between

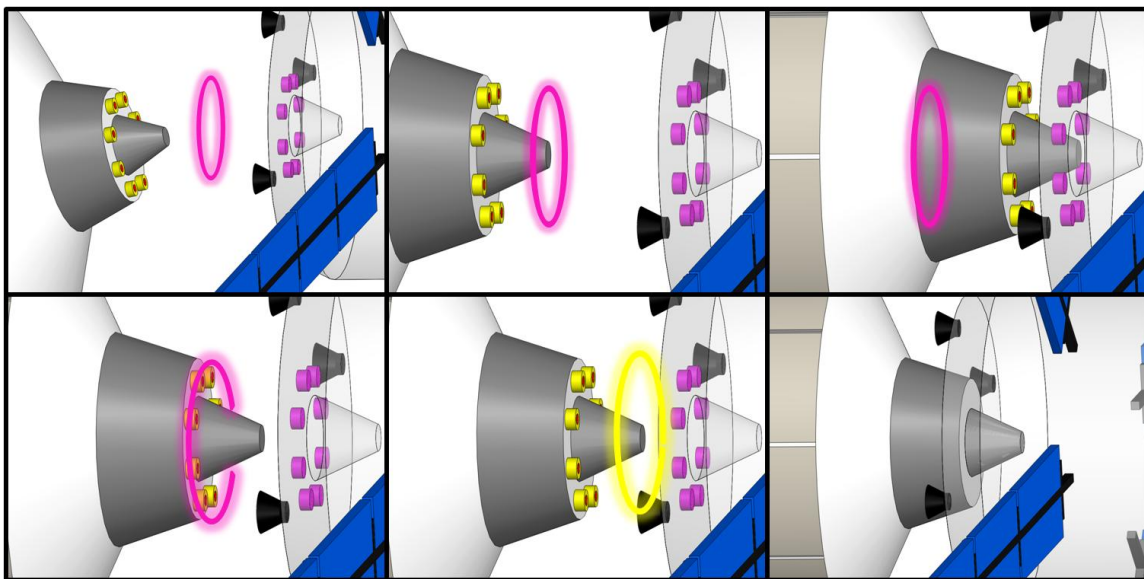


**Figure 2. A conceptual spacecraft with flux-pinned docking augmentation in the six stages of docking, with permanent magnets in red, electromagnets in yellow, and HTSCs in purple. Flux pinning corrects alignment and slows relative velocity of approaching spacecraft (top, left). Magnets draw approaching spacecraft to preset equilibrium within reception range (top, center). Magnets resist collision and damp rebound (top, right). FPI has captured spacecraft at stable equilibrium (bottom, left). Electromagnets activate to draw spacecraft to new, closer equilibrium (bottom, center). Spacecraft deploy physical interface to achieve structural connection (bottom, right)..**

modules.

Though based on the interaction between a magnetic field source and a superconductor, the specific flux-pinned interface used for spacecraft docking can be designed to fit a wide variety of missions. Current demonstrations of flux pinning assisted docking has focused on applications for nanosatellites, specifically CubeSat modules of various sizes. With a cross-sectional area of  $10 \text{ cm}^2$  and a height of 10, 20, or 30 cm, premade standard electronics inserts, and a flexible launching system, the CubeSat platform is ideal for university projects and technology demonstrations. Observations of a 100g Neodymium magnet has been used to characterize the flux pinning interaction with a 56cm diameter single domain superconductor<sup>3</sup>, component sizes that fit well into CubeSat designs. As is show in in Shoer 2008, the dipole moment of a magnet correlates to the magnet's mass. Therefore magnet mass can be used as a significant performance predictor. Magnets in the range shown have noticeable flux pinning effects up to ranges of about 10 cm, with very high stiffnesses as the magnets approach the surface of the superconductor. Though current work has focused on applications in this range of component sizes, the scaling effects observed suggest that larger spacecraft can be augmented with similar performance flux-pinned interfaces by increasing the size of magnet and superconductor components. With FPIs of sufficient strength, flux pinning augmentation could be used to increase the ease and safety of docking on larger spacecraft such as the ATV, illustrated in Figure 3.

### C. Design Parameter Considerations

Implementation of flux-pinned augmentation for docking interfaces will require optimization of the components making up the onboard FPIs. General requirements for spacecraft that will play an important role in flux pinning docking augmentation systems include component mass, power requirements, and volume requirements. Magnet mass has a positive correlation to field strength, so as the forces necessary to make flux pinning useful on a spacecraft of a certain size increase, the magnet mass required to achieve this will likewise increase. Permanent magnets are typically more massive than electromagnets of comparable strength, but the reduced mass of electromagnets come at a cost of increased power requirements. The electromagnets are also more flexible in terms of mission design as their strength and direction can be changed via voltage inputs. Permanent magnets provide a

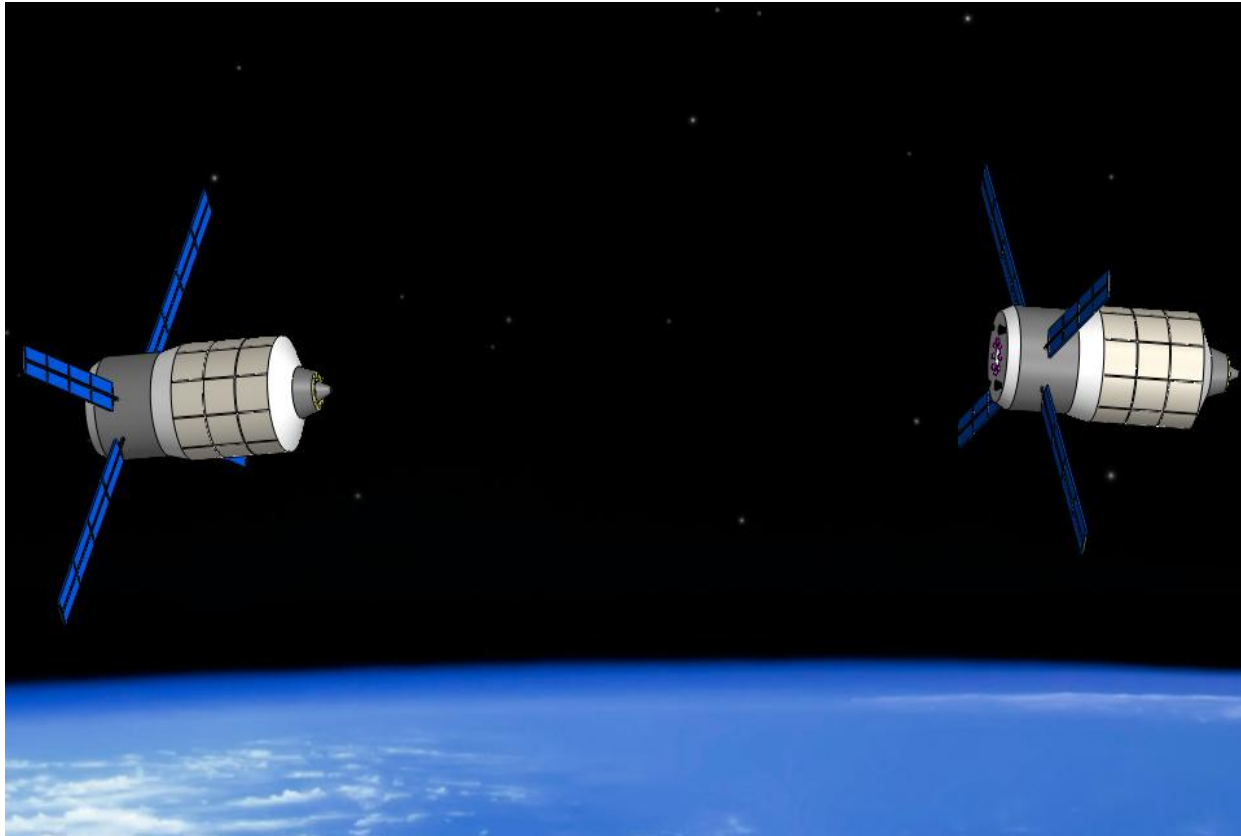


**Figure 3. ATV-like spacecraft docking with flux pinning augmentation.**

more robust failure mode, however, as loss of power will not disengage flux pinning. A combination of permanent magnets surrounded by electromagnetic coils offers the most robust mission performance, as it provides both flexibility (by effectively cancelling the permanent magnet with the electromagnet if so desired) and a safe failure mode, but incurs both a mass and power cost. Magnet volume constrains will typically scale with mass.

Superconductors have, in addition to the aforementioned constraints, parameters defining their pinning strength, critical temperature, and hysteretic effects. The physical makeup of HTSCs define to some degree these properties, with common types such as single domain, thin film, and multi-grain arrays of similar size displaying widely varying behavior. Superconductor size increases with pinning strength, both in planar area and in thickness. These dimensions must be optimized to provide sufficient pinning strength for the specific application while minimizing mass and volume. The critical temperature for superconductors must also be taken into account when designing the FPIs. Though a mission might take advantage of this boundary by allowing the superconductor to warm above  $T_C$  to reset an equilibrium, the HTSC must be kept below this temperature at all other times. In some orbits, a sun shade might be sufficient to achieve this, eliminating any power concerns but imposing an attitude limitation to keep the superconductor out of the sun. When this is not sufficient, the superconductor must be actively cooled, likely by a cryocooler. This will require significant power and spacecraft volume depending on the amount of HTSC

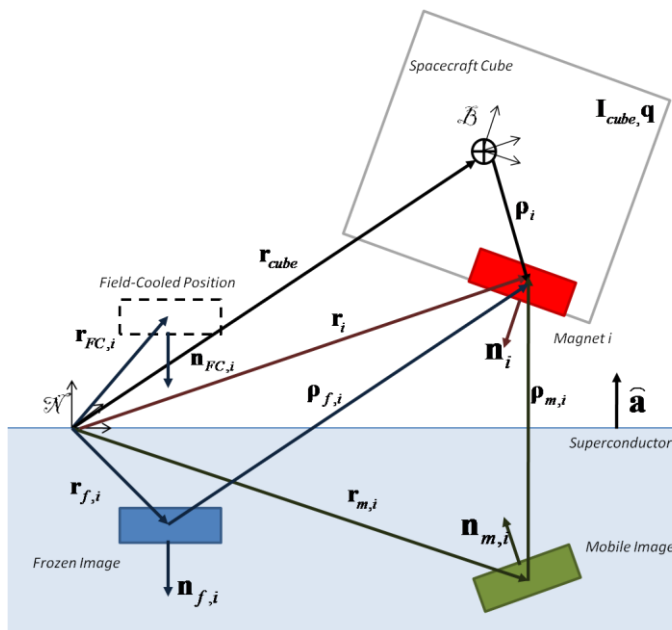


**Figure 5. A generic model of a flux-pinned docking interface, which is based on the Image-Dipole Model as it would be implemented in a spacecraft body.**

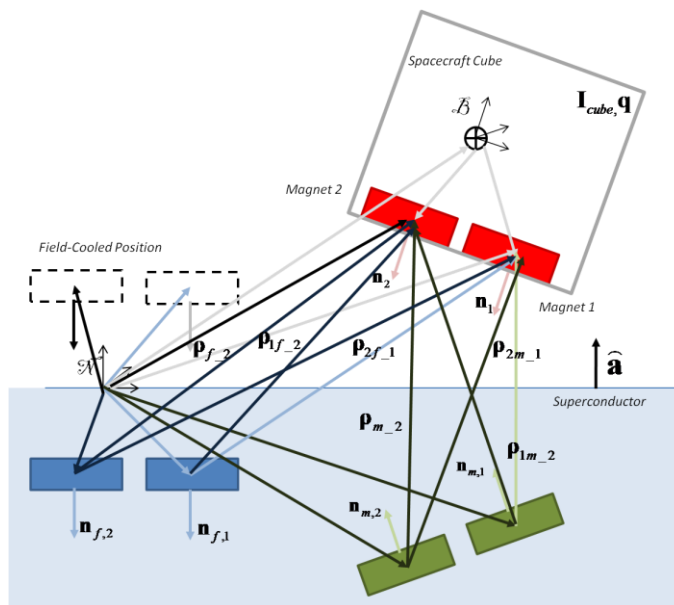


**Figure 4. An augmented model that incorporates two generalized magnets. All of the previously defined vectors have been grayed out, and new vectors from the addition of the second magnet are shown in bold. The new relative vectors are labeled as shown.**

needing to be cooled. Hysteretic effects are also an important design parameter in FPIs. Interfaces designed to keep the equilibrium in a precise position will need to include superconductors with very low hysteresis, such as single grain superconductors. For systems requiring high hysteresis, one option would be in use thin film superconductors that naturally exhibit this behavior.

Other ways of changing a flux-pinned interface to better suit a mission include adding additional materials around the magnets and superconductors. Introducing aluminum will significantly increase the damping experienced by the system, which could be desirable to reduce vibrations. Adding ferrous material will increase the range of magnetic attraction between two modules. These and the previously mentioned options provided many ways to customize the basic magnet-superconductor interaction to suit a wide variety of spacecraft docking missions.

### III. Flux-Pinned Docking Interface Validation

#### A. Flux-Pinned Docking Interface Model

Traditional flux pinning studies have focused on characterizing the relationship between manufacturing techniques and the characteristics of the flux pinning, such as hysteretic effects,<sup>16</sup> improving the lateral stiffness for levitation applications,<sup>17</sup> and exploiting non-stiff degrees of freedom for bearing applications<sup>18</sup>. For the purposes of this paper, the flux pinning considered is caused by field-cooling the superconductor in the presence of a dipole magnetic field with negligible hysteretic and edge effects. Kordyuk's Image-Dipole Model (IDM) uses a series of dipole "images" reflected over the surface of the superconductor to approximate the effect of flux pinning under these assumptions. The summation of the magnetic fields of the images then produces a set of forces and torques on the magnetic field source that act to restore the system to its field-cooled position.<sup>19</sup>

The IDM produces two images for every magnetic dipole field-cooled near the superconductor: a frozen image and a mobile image. The frozen image is formed by the magnet in its field-cooling position, and is modeled by reflecting the position over the surface of the superconductor and negating the orientation such that the magnet and its frozen image tend to attract. The mobile image, on the other hand, follows the position of the magnet reflected over the superconductor's surface with an orientation that tends to repel its source magnet. At the field-cooled equilibrium, the mobile image and frozen image cancel out and thus exert no force or torque on the source magnet. A model of how this model applies to a spacecraft, including nomenclature and variables, is shown in Figure . For this paper, bold face represents vectors, a hat represents a unit vector, and italics indicate a scalar variable.

This model approximates the nonlinear potential well experienced by a flux-pinned magnet. Additional magnets, such as actuating electromagnets, can be included in this model either field cooled into the superconductor (where their frozen image will appear as described above), or not field-cooled into the superconductor, where only the mobile image will affect the system dynamics. In either case, the images of all magnets exert forces and torques on all other source magnets in the system, as suggested by the nomenclature in Figure 4.

Using expressions for the reflected vectors for the mobile and frozen images<sup>3</sup> and the general equations for the force and torque caused by one magnet on the other,<sup>20</sup> the expressions for the force and torque exerted on source magnet 1 by its mobile image is:

$$\mathbf{F}_{1m-1} = \frac{3\mu_0 n_{m-1} n_1}{4\pi\rho_m^4} \left[ \hat{\rho}_m (\hat{n}_{m-1} \cdot \hat{n}_1) + \hat{n}_{m-1} (\hat{\rho}_m \cdot \hat{n}_1) + \hat{n}_1 (\hat{\rho}_m \cdot \hat{n}_1) - 5\hat{\rho}_m (\hat{\rho}_m \cdot \hat{n}_{m-1}) (\hat{\rho}_m \cdot \hat{n}_1) \right] \quad (1)$$

$$\mathbf{T}_{1m-1} = \frac{\mu_0 n_{m-1} n_1}{4\pi\rho_m^3} \left[ 3(\hat{n}_{m-1} \cdot \hat{\rho}_m) (\hat{n}_1 \times \hat{\rho}_m) + (\hat{n}_{m-1} \times \hat{n}_1) \right]$$

where the magnetic dipole moment vector for the mobile image can be described by:

$$\mathbf{n}_{m-1} = (\mathbf{n}_1 - 2(\hat{\mathbf{a}} \cdot \mathbf{n}_1)\hat{\mathbf{a}}) \quad (2)$$

Similar expressions can be derived for the frozen image's effect, using the magnetic dipole vector:

$$\mathbf{n}_{f-1} = 2(\hat{\mathbf{a}} \cdot \mathbf{n}_{FC})\hat{\mathbf{a}} - \mathbf{n}_{FC} \quad (3)$$

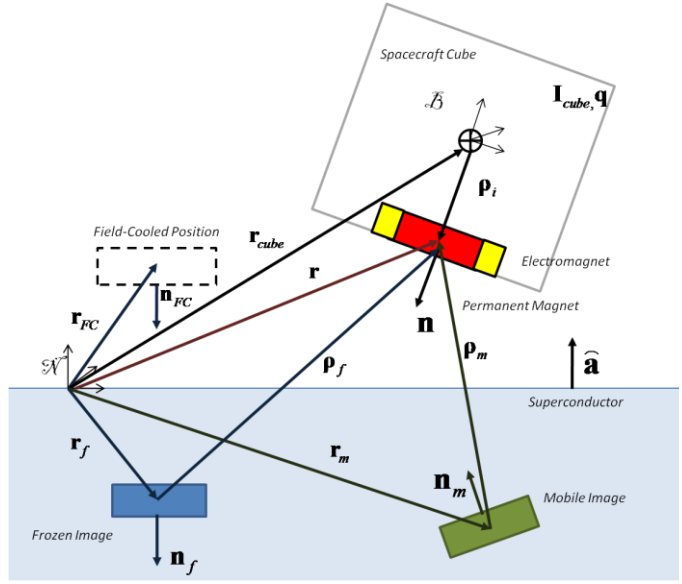


**Figure 6. A more specific model that treats a collocated permanent magnet and electromagnet as one magnet with a varying magnetic field strength.**

The subscript  $FC$ , as in Shoer's 2010 paper, represents the quantity at field cooling. Cross-coupling between source magnets and the images of other magnets can be found using the appropriate dipole magnet vectors and the relative position between the images and the source magnet. For example, the effect of magnet 2's mobile image on magnet 1 can be described in the following equation:

$$\mathbf{F}_{2m-1} = \frac{3\mu_0 n_{2m-1} n_1}{4\pi\rho_{2m-1}^4} \left[ \hat{\rho}_{2m-1} (\hat{\mathbf{n}}_{2m-1} \cdot \hat{\mathbf{n}}_1) + \hat{\mathbf{n}}_{2m-1} (\hat{\rho}_{2m-1} \cdot \hat{\mathbf{n}}_1) + \hat{\mathbf{n}}_1 (\hat{\rho}_{2m-1} \cdot \hat{\mathbf{n}}_1) - 5\hat{\rho}_{2m-1} (\hat{\rho}_{2m-1} \cdot \hat{\mathbf{n}}_{2m-1}) (\hat{\rho}_{2m-1} \cdot \hat{\mathbf{n}}_1) \right] \quad (4)$$

where the relative position of the mobile image of magnet 2 and magnet 1 is:

$$\boldsymbol{\rho}_{2m-1} = \mathbf{r}_1 - \mathbf{r}_{m2} = \mathbf{r}_{cube} + \boldsymbol{\rho}_1 - (\mathbf{r}_2 - 2(\hat{\mathbf{a}} \cdot \mathbf{r}_2)\hat{\mathbf{a}}) \quad (5)$$

The model described above works for general flux-pinned systems within the assumptions of the dipole moments and infinite superconductors. To understand the dynamics of a Flux-Pinned Docking Interface as described earlier, however, a more specific model is used (as shown in Figure 6). In this model, an electromagnet (shown in yellow) wraps around a permanent magnet (shown in red), both of which are placed directly in the center of the module to which they are attached. Because the permanent magnet and electromagnet dipoles are co-located, the mobile images add together directly as one image with a varying magnetic dipole strength. Similarly, the frozen image is either attenuated or augmented by the electromagnet (depending on the direction of the electromagnet's dipole vector). If the electromagnet is off during the field cooling process, the frozen image of the permanent magnet remains.

## B. System Parameters

The system parameters for the simulations below are based on the microgravity flight hardware for the Robust Autonomous Grapppler for Noncontacting Actuation and Reconfiguration (RAGNAR) project, which is being developed by the Cornell Space Systems Design Studio for NASA's Facilitated Access to the Space Environment for Technology (FAST) program. The experiment dates are the week of Sept. 27<sup>th</sup> – Oct. 1<sup>st</sup>.

The experiment involves two CubeSat-sized modules (12.5 cm cubes of approximately 3 kg) that are equipped with a Flux-Pinned Docking Interface. The superconductor will be cooled in between microgravity parabolas via an onboard cryocooler. Each module contains an onboard autonomous microcontroller and an IMU package, and the Xbee communications architecture between the cubes allows them to share their relative position and orientation with one another. One of the modules contains a series of permanent magnets and electromagnets which will form the other half of the Flux-Pinned Docking Interface. This cube will be capable of using the relative position and orientation values from the cubes to autonomously control its equilibrium position. Figure 7 shows the two cubes and the flux-pinned interface between them.

The inertia values, system geometry, and magnet strengths in the simulation are all based on estimates from this hardware setup. Damping ratios are based on conservative estimates from previous experimental data,<sup>3</sup> (on the order of 0.02) with the expectation that the addition of aluminum to the Flux-Pinned Docking Interface can add eddy-current damping if higher damping ratios are desired. The field-cooling distance is assumed to be 1 cm, which is within the expectations for the experimental setup of this nature. Assuming the magnets are located 5 cm from the center of mass of the cube, the equilibrium position will be (0, 0, 6) in centimeters. Docking separation distances are anticipated to be on the order of a few centimeters.

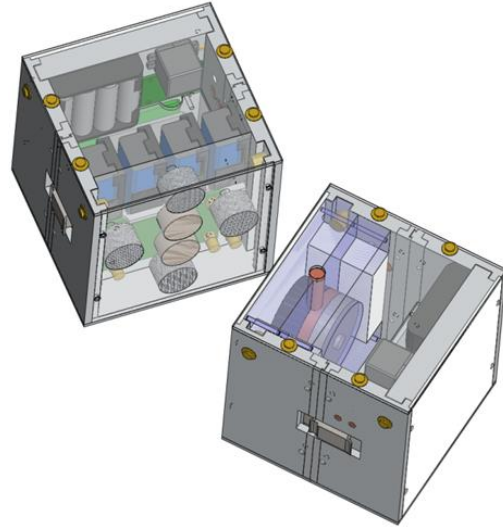


**Figure 7. A more specific model that treats a collocated permanent magnet and electromagnet as one magnet with a varying magnetic field strength.**

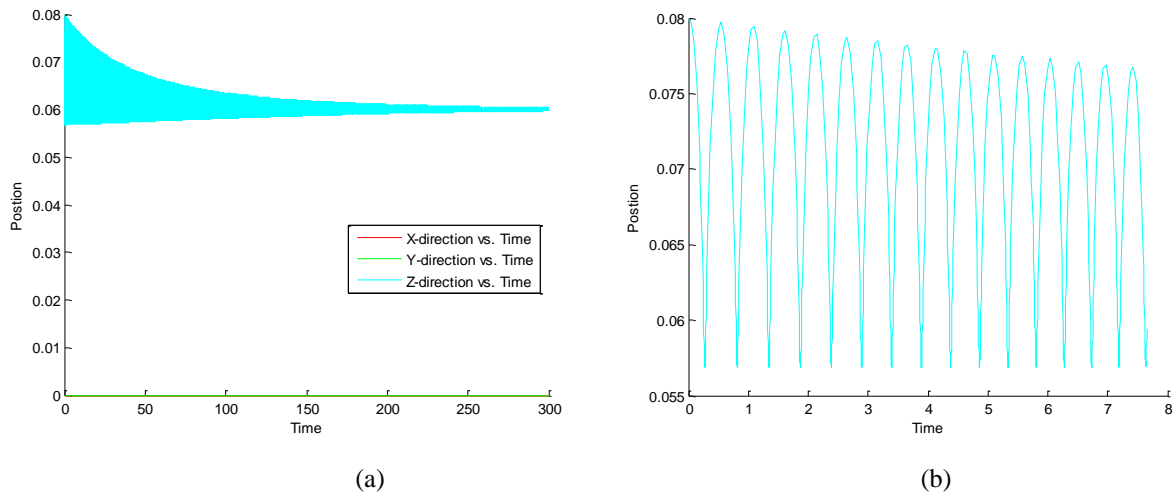


**Figure 9. A plot of the position (in meters) for a simple Flux-Pinned Docking Interface with no voltage in the electromagnet, starting from displaced position two centimeters offset in the z direction. (a) Is a full view, with a conservative damping ratio, showing the system fully damping out on the order of minutes, and (b) is a zoomed-in view of the oscillations, which shows the nonlinear behavior of the system about its equilibrium of 0.06 m.**

### C. Passive System Dynamics

In a permanent magnet/electromagnet collocated model described above, the system’s passive dynamics (where the electromagnet is given a constant voltage which is not varied for the duration of the maneuver) are indicators of how the system will behave in the event of a complete control system failure (the electromagnet freezes at a given voltage). For example, Figure 8 shows the case where no voltage is applied. With a low damping coefficient, the system damps out to its equilibrium within a few minutes. The system is clearly stable in the control-failure case, with the nonlinear damping affects clear in the way that the system has much sharper responses to going closer to the superconductor than its equilibrium position. The high stiffness of the system is due to the strong magnets and relatively low mass involved. When the electromagnet is fixed at 10 V, the system also remains stable, as shown in Figure 9.

## IV. Conclusion

One of the most important and currently hazardous stages of spacecraft docking is close range rendezvous. Flux pinned interfaces can significantly increase the safety of this maneuver and simplify its operation by taking advantage of the magnetic flux pinning interaction. This docking augmentation method is currently being demonstrated in both simulation and microgravity flight at the nanosatellite scale but can likely be scaled up to work on larger spacecraft by increasing the size of the FPI components. Some of the parameters important for optimization when designing a flux-pinned docking augmentation system include component mass, volume, power requirements, and superconductor behavior. Systems with different costs and capabilities can be designed for specific applications to match their behavior with desired performance. The system has shown in simulation to be resistant to collisions even in the control failure case, and can be easily actuated with inputs to the

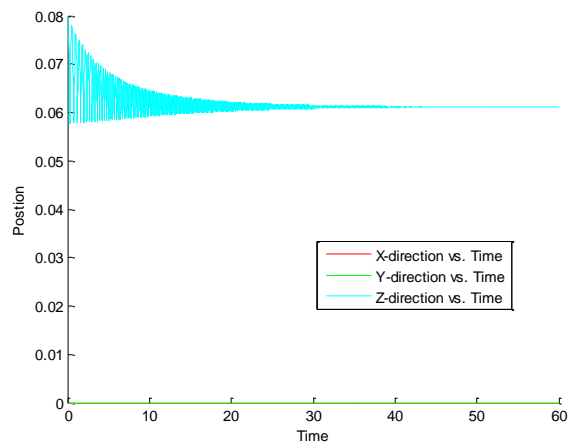


**Figure 8. Increasing the damping ratio slightly and including a failure case where the electromagnet is fixed at 10 V, and the system remains stable at its equilibrium.**

electromagnets. This docking augmentation method offers a promising array of features that would be very beneficial to the future of spacecraft rendezvous systems, and the experiments set to occur at the end of September 2010 have the potential to raise the TRL of this technology to a level that makes its implementation on actual space systems much closer to reality.

### Acknowledgments

L. Jones would like to thank the National Defense Science and Engineering Graduate Fellowship program for funding this work, Joseph Shoer and Jillian Gorsuch for their work on this project, and the rest of the members of the Space Systems Design Studio at Cornell University.

### References

- 
- <sup>1</sup> Fehse, Wigbert, *Solar Autonomous Rendezvous and Docking of Spacecraft*, University of Cambridge, Cambridge, UK, 2003.
  - <sup>2</sup> Davis, L. C., Logothetis E. M., and Soltis, R. E., "Stability of Magnets Above Superconductors," *Journal of Applied Physics*, Vol. 64, No. 8, 1988, pp. 4212-4218.
  - <sup>3</sup> Shoer, J., and Peck, M. "Flux-Pinned Interfaces for the Assembly, Manipulation, and Reconfiguration of Modular Space Systems," *AIAA Guidance, Navigation, and Control Conference*, August 2008.
  - <sup>4</sup> Jones, L., and Peck, M. "Stability and Control of a Flux-Pinned Spacecraft Docking Interface," *AIAA Guidance, Navigation, and Control Conference*, August 2010.
  - <sup>5</sup> Shoer, J., Wilson, W., Jones, L., Knobel, M., and Peck, M. "Microgravity Demonstrations of Flux Pinning for Station-Keeping and Reconfiguration of CubeSat-Sized Spacecraft," *Journal of Spacecraft and Rockets* (Accepted pending revisions).
  - <sup>6</sup> Wilson, W. and Peck, M. "An Air-Levitated Testbed for Flux Pinning Interactions at the Nanosatellite Scale," *AIAA Modeling and Simulation Technologies Conference*. AIAA, Toronto, 2010.
  - <sup>7</sup> Schonhuber, P. and Moon, P. C., "Levitation forces, stiffness, and force-creep in YBCO high-Tc superconducting thin films," *Applied Superconductivity*, Vol. 2, No. 7, 1994, pp. 523-534.
  - <sup>8</sup> Davis, L. C., "Lateral restoring force on a magnet levitated above a superconductor," *Journal of Applied Physics*, Vol. 67, No. 5, 1990, pp. 2631-2636.
  - <sup>9</sup> Kramer, E. J., "Scaling laws for flux pinning in hard superconductors," *Journal of Applied Physics*, Vol. 44, No. 3, 1973, pp. 1360-1370.
  - <sup>10</sup> Brandt, E. H., "Rigid levitation and suspension of high-temperature superconductors by magnets," *American Journal of Physics*, Vol. 58, No. 1, 1990, pp. 43-49.
  - <sup>11</sup> Shoer, J. and Peck, M. "Reconfigurable Spacecraft as Kinematic Mechanisms Based on Flux-Pinning Interactions," *Journal of Spacecraft and Rockets*, Vol. 46, No. 2, 2009, pp. 466-469.
  - <sup>12</sup> Wilson, W., Shoer, J., and Peck, M., "Demonstration of a Magnetic Locking Flux-Pinned Revolute Joint for Use on CubeSat-Standard Spacecraft." *AIAA Guidance, Navigation and Control Conference and Exhibit*. AIAA, Chicago, 2009.
  - <sup>13</sup> Wilson, W. "Results of Flux-Pinned Modular Spacecraft Demonstration in Microgravity." *AIAA Region I Young Professional and Student Conference*, Laurel, MD, 2009.
  - <sup>14</sup> "Rendezvous and Docking Technology", ATV Information Kit, [www.esa.com](http://www.esa.com). Accessed 8/7/2010.

---

<sup>15</sup> “Overview of the DART Mishap Investigation Results,” Online, Internet. Accessed Jan 2010. Available at < [http://www.nasa.gov/pdf/148072main\\_DART\\_mishap\\_overview.pdf](http://www.nasa.gov/pdf/148072main_DART_mishap_overview.pdf) >.

<sup>16</sup> Hogg, Michael J., Kahlmann, Frank, Barber, Zoe H., and Evetts, Jan E., “Angular hysteresis in the critical current of YBa<sub>2</sub>Cu<sub>3</sub>O<sub>7</sub> low-angle grain boundaries,” *Superconductor Science and Technology*, Vol. 14, 2001, pp. 647-650.

<sup>17</sup> Davis, L. C., “Lateral Restoring Force on a Magnet Levitated above a Superconductor,” *Journal of Applied Physics*, Vol. 67, No. 5, 1990, pp. 2631-2636.

<sup>18</sup> Ma, K. B., Postrekhin, Y. V., and Chu, W. K., “Superconductor and magnet levitation devices,” *Review of Scientific Instruments*, Vol. 74, No. 12, Dec. 2003, pp. 4989-5017.

<sup>19</sup> Kordyuk, A., “Magnetic levitation for hard superconductors,” *Journal of Applied Physics*, Vol. 83, No. 1, 1998, pp. 610-612.

<sup>20</sup> Yung, K. W., Landecker, P. B., and Villani, D.D., “An Analytic Solution for the Force Between Two Magnetic Dipoles,” *Magnetic and Electrical Separation*, Vol. 9, 1998, pp. 39-52.